Nature Environment and Pollution Technology
An International Quarterly Scientific Journal

p-ISSN: 0972-6268
(Print copies up to 2016)
e-ISSN: 2395-3454

Vol. 25 | No. 2 | Article ID D1821 | 2026

Original Research Paper

https://doi.org/10.46488/NEPT.2026.v25i02.D1821

Open Access Journal

Mathematical Modeling of Oxygenation Capacity in Wastewater Based on Air Diffuser Type

Arlitt Amy Lozano Povis[1], Oscar Sedano Vargas[2], Joel Colonio Llacua[1] and Elvis Carmen Delgadillo[1]†

[1]Faculty of Engineering, Continental University, Avenida San Carlos 1980, San Antonio Urbanization, Huancayo, Peru
[2]Graduate School, Continental University, Avenida San Carlos 1980, Huancayo, Peru
†Corresponding author: Elvis Carmen Delgadillo; ecarmen@continental.edu.pe

Abbreviation: Nat. Env. & Poll. Technol.
Website: www.neptjournal.com

Received: 20-05-2025
Revised: 15-07-2025
Accepted: 03-08-2025

Key Words:

Predictive models
Oxygenation kinetics
Diffusion aeration
Biological reactors

Citation for the Paper:

Lozano Povis, A.A., Sedano Vargas, O., Colonio Llacua, J. and Carmen Delgadillo, E., 2026. Mathematical modeling of oxygenation capacity in wastewater based on air diffuser type. *Nature Environment and Pollution Technology*, 25(2), D1821. https://doi.org/10.46488/NEPT.2026.v25i02.D1821

Note: From 2025, the journal has adopted the use of Article IDs in citations instead of traditional consecutive page numbers. Each article is now given individual page ranges starting from page 1.

ABSTRACT

The oxygenation capacity in wastewater directly affects the performance of biological treatment systems. In this context, this study develops a mathematical model that describes this capacity as a function of the aeration system used. Three configurations were evaluated: fine bubble, coarse bubble, and extra coarse bubble, using experimental tests that measured dissolved oxygen concentration, saturation time, and the overall mass transfer coefficient (kLa). The resulting models achieved high fit (R^2 between 0.9988 and 1), supporting their validity in representing the observed behavior. The fine bubble system showed the highest initial oxygenation capacity, reaching 1.28 $mg.L^{-1}.s^{-1}$, though it decreased significantly over time by 96.09%. Overall, the results quantitatively characterize the dynamics of each diffuser type, providing relevant technical criteria for the design and selection of wastewater treatment systems.

INTRODUCTION

Wastewater contains a wide range of contaminants, including organic matter, nutrients, heavy metals, toxic chemicals, and pathogens. If not effectively treated, these contaminants pose a potential threat to aquatic ecosystems, water quality, and human health (Dey et al. 2022, Xu & Xu 2022). Physical, chemical, and biological processes are employed to remove them (Pang et al. 2020).

Among these, biological methods such as aeration offer a more sustainable and efficient alternative compared to physical and chemical treatments, which often involve higher operational costs and generate unwanted byproducts. This treatment is particularly suitable for small- and medium-scale domestic wastewater treatment plants. It operates by supplying oxygen to the wastewater through pipes that release air bubbles, promoting mass transfer at the air-water interface. As a result, aerobic microorganisms can effectively degrade the organic matter present (Cheng et al. 2016, Dyagelev et al. 2021, Lebrun et al. 2022).

However, despite its wide applicability, significant gaps remain in understanding the factors affecting its efficiency. Aspects such as system geometry, diffuser type, bubble size, dissolved oxygen concentration, and dynamic flow conditions can significantly influence process performance. Mathematical modeling emerges as a key tool to address these limitations, enabling the simulation of system behavior under different scenarios without costly or hard-to-control physical tests (Cao et al. 2017, Farazaki & Gikas 2019, Hocaoglu et al. 2011, Ma et al. 2017).

These predictive models allow the analysis of critical variables, optimization of operational parameters, and improvement of system design. However, many remain generalized and require specific validations for conditions (Arora-Jonsson 2023, Levitsky et al. 2022, Lu et al. 2021).

In this context, this study aimed to model the oxygenation capacity in domestic wastewater, considering three key variables: diffuser type, overall mass transfer coefficient, and aeration time. The results can be applied to both the design of new treatment plants and the optimization of existing facilities, contributing to improved energy efficiency and treated effluent quality in urban and rural settings.

MATERIALS AND METHODS

Components of the Experimental Unit and Sample Preparation

Data collection involved oxygenation tests on synthetic domestic wastewater samples using a specially designed experimental unit. The system included an air compressor as the primary oxygen source, connected via a 10 mm inner-diameter transparent plastic hose. A pressure regulator and a 1/4" needle valve were incorporated to precisely control the flow rate.

For monitoring relevant variables, a PT100 temperature sensor (measurement range: -50°C to 150°C, accuracy: ±0.1°C) and a dissolved oxygen sensor (range: 0 to 20 ppm, accuracy: ±0.1 ppm) were integrated. A 1" ball valve was installed at the bottom of the container to facilitate drainage and cleaning between tests (Fig. 1).

Once assembled, 36 liters of domestic wastewater were prepared. For this, 5 g of peptone was added to provide organic nitrogen, peptides, and amino acids for protein synthesis and cell development. As the primary energy source, 1.2 g of sucrose was incorporated, while 2.8 g of starch provided sustained carbon release. Additionally, 1 g of soybean oil was added to supply lipids and essential fatty acids for cell membrane formation. The inclusion of 0.6 g of ammonium sulfate met inorganic nitrogen requirements, favoring amino acid synthesis. Finally, 0.12 g of tribasic sodium phosphate was added as a pH regulator and phosphorus source, a key element in metabolic and structural functions.

Wastewater Deoxygenation

To begin the experiments, sodium sulfite (Na_2SO_3) and its catalyst, cobalt chloride ($CoCl_2$), were added to reduce the dissolved oxygen concentration to zero, according to the following reaction:

$$Na_2SO_3 + \frac{1}{2}O_2 \xrightarrow{CoCl_2} Na_2SO_4$$

Considering the stoichiometric ratio:

$$\frac{Na_2SO_3}{\frac{1}{2}O_2} = \frac{126{,}043\,\frac{g}{mol}}{32\,\frac{g}{mol}} = 3.94$$

Based on this value, the required amount of subscript base, cap N a, end base, sub 2, subscript base, cap S, cap O, end base, and sub 4 was calculated, with a 20% excess to ensure complete dissolved oxygen removal. The mixture was stirred for 5 min with a stainless-steel rod to ensure homogeneous reagent distribution. The compressor was then activated to begin the oxygenation process, which is essential for adequate oxygen transfer. This procedure was repeated for each evaluated air diffuser type.

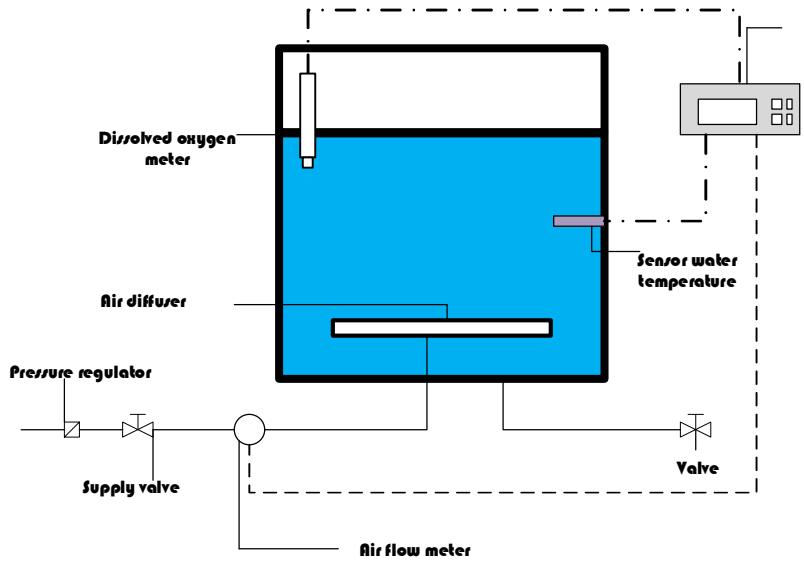

Fig. 1: Schematic of the experimental unit used for oxygenation tests in synthetic wastewater.

Calculation of Mass Transfer Coefficient and Oxygenation Capacity

The volumetric mass transfer coefficient (k_La) required a mathematical approach based on the temporal behavior of dissolved oxygen concentration.

Oxygen Transfer Equation (Exponential Model)

This dynamic was described using an exponential model proposed by Levitsky et al. (2022), expressed by Equation (1):

$$C_L = C_S - (C_S - C_O).e^{-K_La.(t_2-t_1)} \quad \ldots(1)$$

Where C_L represents dissolved oxygen concentration at time t, C_S the saturation concentration, C_O the initial concentration, and k_La the mass transfer coefficient. Expressed differentially, Equation (2) is obtained:

$$\frac{dc}{dt} = k_La(C_s - C) \quad \ldots(2)$$

Rearranging the above expression yields an integrable form facilitating experimental calculation of k_La, presented in Equation (3):

$$\frac{dc}{(C_s-C)} = k_La(d_t) \quad \ldots(3)$$

Integration of the Equation to Obtain

To determine k_La, the oxygen transfer differential equation (Equation 3) was used. Considering that at t = 0, oxygen concentration is C_i, and at time t, it increases to C_t, both sides of the equation were integrated:

$$\int_{C_i}^{C_t} \frac{dc}{c_s-c_L} = \int_0^t k_La(dt) \quad \ldots(4)$$

This expression allows solving for the coefficient k_La as a function of time and initial and final dissolved oxygen concentrations, yielding the following logarithmic relation (Equation 5):

$$\ln\left[\frac{C_s-C_i}{C_s-C_t}\right] = k_La.t \quad \ldots(5)$$

Rearranged equivalently:

$$\ln[C_s - C_t] = \ln[C_s - C_i] - k_La.t \quad \ldots(6)$$

Thus, k_La was determined via linear regression of experimental data.

Relation to Oxygenation Capacity

Oxygenation capacity represents the amount of oxygen transferred per unit volume and time, calculated using Equation 7:

$$N = k_La\ (C_S - C_L) \quad \ldots(7)$$

Where N is oxygenation capacity (mg O_2/L min), k_La is the mass transfer coefficient (min^{-1}), C_s is oxygen saturation concentration in the system (mg/L), and C_L is the dissolved oxygen concentration at time t.

Data Processing

Measurements were organized by bubble type: fine, coarse, and extra coarse. Interpolation and surface-fitting techniques were used to construct a 3D mesh representing the combined behavior of time, mass transfer coefficient (kLa), and oxygenation capacity.

For visualization, R was used with 3D graphics libraries. Response surfaces were color-coded by bubble type: red and yellow for fine bubbles, blue and yellow for coarse bubbles, and purple-green-yellow for extra coarse bubbles. The graph featured three axes: x-axis for time (min), y-axis for mass transfer coefficient (kLa), and z-axis for oxygenation capacity (mg/L).

R was also used for linear regression to calculate mass transfer coefficients (kLa), polynomial model fitting by diffuser type and operation time, and ANCOVA to statistically evaluate the effects of bubble type, time, and their interaction on system efficiency. To ensure statistical reliability, each experimental run for the different diffuser configurations was performed in triplicate.

RESULTS AND DISCUSSION

Dissolved Oxygen Concentration

Fig. 2 shows dissolved oxygen concentration evolution over time at 0.5-second intervals. The fine bubble diffuser reached saturation in 18.5 min, while coarse and extra coarse bubble diffusers took 72 and 64 min, respectively. Global average temperature was 16.1°C ±0.249. ANOVA by diffuser type showed significant differences favoring fine bubble diffusers in average time to maximum oxygen concentration (ANOVA $p < .001$, Shapiro normality test $p < .001$).

The fine bubble diffuser achieved saturation faster than coarse or extra coarse bubble diffusers, aligning with prior studies reporting higher efficiency in oxygen transfer per unit time (Newbry 1998, Rosso & Stenstrom 2006). Herrmann-Heber et al. (2020, 2021) recorded 98% dissolved oxygen concentration in 10.25 min under constant flow, while unagitated liquid systems may require significantly longer equilibration times (Ghodke & Vishal Reddy 2023).

Mass Transfer Coefficient (

Fig. 3 presents k_La values adjusted per Equation (5): 0.25 for fine bubbles, 0.049 for coarse bubbles, and 0.056 for extra coarse bubbles.

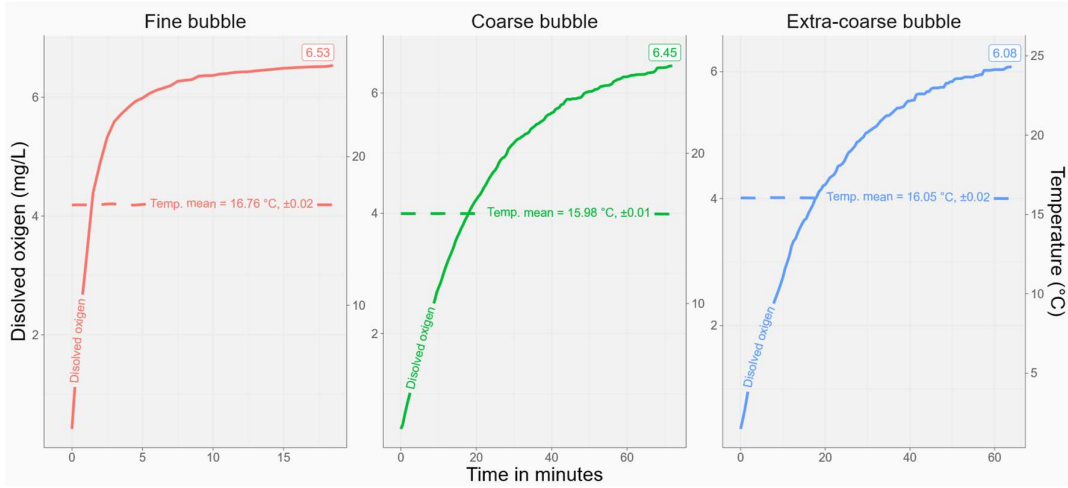

Note. Maximum time FB = 18.5 min, CB = 72 min, ECB = 64 min. ANOVA p < .001. Global average maximum dissolved oxygen = 6.36 ±0.24. Global average temperature = 16.1 °C ±0.249.

Fig. 2: Dissolved oxygen concentration.

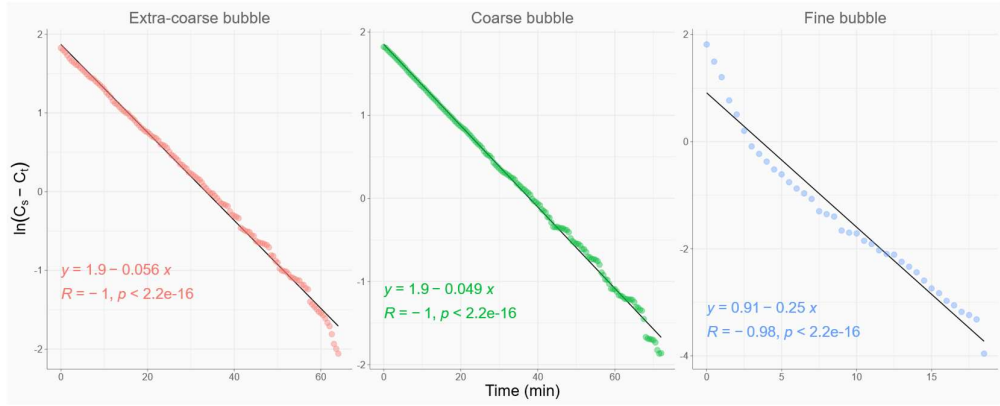

Fig. 3: Regression curves for determining $k_L a$.

Higher kLa values for fine bubbles align with literature, where smaller bubbles generate greater gas-liquid interfacial area, enhancing oxygen transfer efficiency (Asselin et al. 1998, Gillot et al. 2005, Skouteris et al. 2020). Elevated kLa indicates better medium oxygenation (Reshma et al. 2021).

It is important to note that the oxygen transfer rate is directly influenced by the surface area to volume (S/V) ratio of the system. While this study did not explicitly calculate the gas-liquid interfacial area, the superior performance of the fine bubble diffuser is qualitatively consistent with this principle. The generation of smaller bubbles creates a significantly larger total surface area for a given volume of air, thereby increasing the S/V ratio and enhancing the driving force for mass transfer. The consistent experimental geometry (36 L volume and 35 cm liquid depth) ensures that the observed differences are primarily attributable to the diffuser characteristics. This is a key factor that should be quantitatively explored in future studies.

While this study did not implement an airlift recirculation system, its potential for future applications is noteworthy. Such systems can increase activated sludge concentration and improve suspended solids distribution, potentially boosting dissolved oxygen by 15% and mass transfer reactions by 11.8% (Khalil & Sharshir 2022). Industrial studies show fine-slot disc diffusers can triple oxygen transfer efficiency in saline media compared to conventional configurations (Behnisch et al. 2022), suggesting relevant improvements for aeration systems like this study's.

Oxygenation Capacity

Oxygenation capacity (OC) was calculated using Equation 7, generating curves describing OC behavior by diffuser type

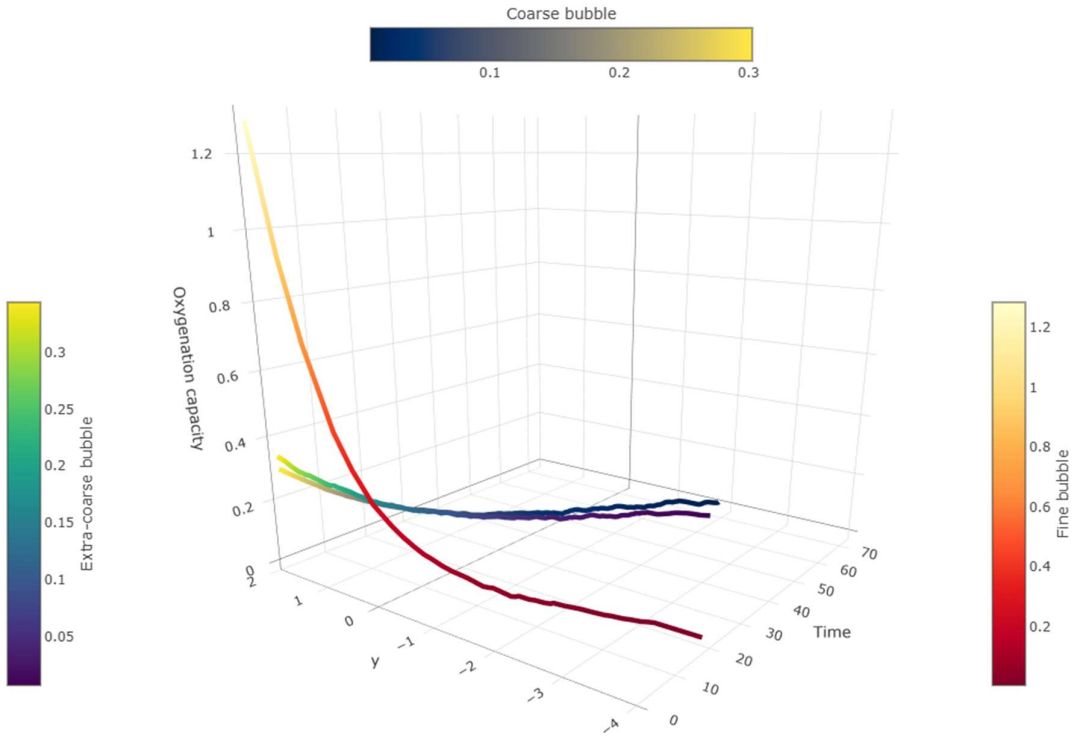

Fig. 4: Oxygenation capacity vs time. y = ln (Cs - Ct).

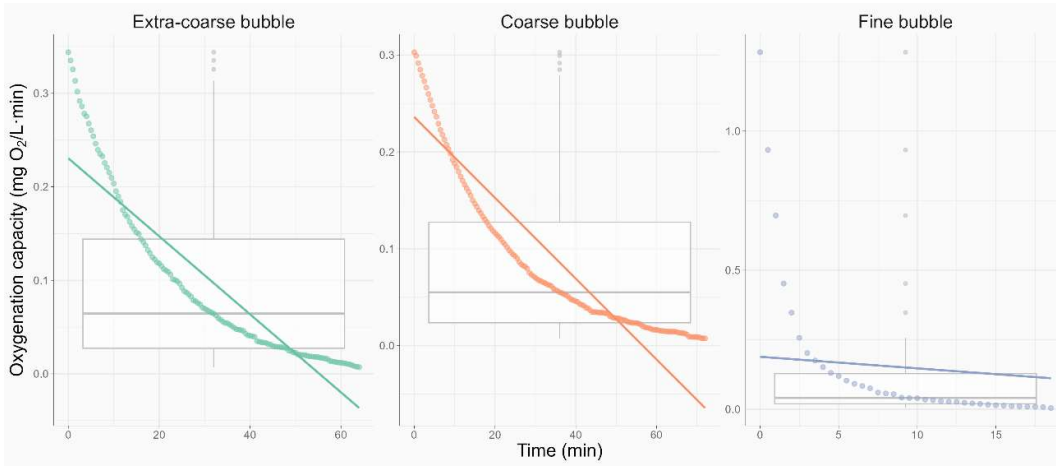

Fig. 5: Oxygenation capacity differences by time and diffuser type.

over time t (Fig. 4). Curves showed a descending trend as OC decreases toward oxygen saturation, indicating higher efficiency in early min. The fine bubble diffuser achieved a maximum OC of 1.28 mg.L^{-1}, significantly outperforming coarse (0.30 mg.L^{-1}) and extra coarse (0.34 mg.L^{-1}) diffusers.

Between 5-10 min, values approached 2.0 mg.L^{-1}, representing the optimal operation range before stabilization. Color transition (red, yellow) visually reinforces this trend. Extra coarse bubbles showed flatter, lower surfaces (purple, green), evidencing low efficiency, not exceeding 0.8 mg.L^{-1} even at process end, suggesting limited oxygen transfer over time.

Fig. 5 and Table 1 show time and diffuser type interactions on OC. ANCOVA showed significant OC differences by diffuser type (Table 1, $p < .001$), demonstrating OC's dependence on time and diffuser type.

Table 1: Covariance analysis results.

	Df	Sum Sq	Mean Sq	F value	Pr(>F)
Time	1	1.970035	1.970035	342.0105	8.70E-52
Diffuser type	2	0.05783	0.028915	5.019829	0.00716
Time:Diffuser	2	0.984258	0.492129	85.43674	3.31E-30
Residuals	306	1.762609	0.00576		

Table 2: Polynomial regression equations by diffuser type.

Diffuser Type	Mathematical Model	R^2
Fine bubble	$y = 1.2781 - 0.81339x + 0.22821x^2 - 0.03277x^3 + 0.0025x^4 - 9.61937E\text{-}5x^5 + 1.47022E\text{-}6x^6$	1
Coarse bubble	$y = 0.30323 - 0.01496x + 3.64529E\text{-}4x^2 - 5.29557E\text{-}6x^3 + 4.36382E\text{-}8x^4 - 1.57334E\text{-}10x^5$	0.999
Extra coarse bubble	$y = 0.33975 - 0.01607x + 2.90008E\text{-}4x^2 - 1.89363E\text{-}6x^3$	0.998

Polynomial Model Fitting

To characterize OC evolution over time, polynomial models were fitted for each diffuser type, with time as the independent variable. The fine bubble model fit a sixth-degree polynomial with $R^2 = 1$, indicating perfect experimental data correspondence (Table 2).

The use of a high-degree polynomial for the fine bubble system, yielding an R^2 of 1, warrants a discussion of model validity. While this indicates an excellent descriptive fit for the collected data in our controlled experimental setup, it also raises concerns about overfitting. A model that perfectly fits the training data may not generalize well to new, unseen data. For future studies, it would be beneficial to apply techniques such as cross-validation or to evaluate alternative, less complex models (e.g., exponential or mechanistic models) to ensure the development of a robust predictive tool that avoids overfitting.

Nonlinear responses, especially for fine bubbles, reflect complex, unstable bubble dynamics in liquids, causing abrupt variations in oxygenation rates. Coarse bubble models showed more regular, predictable behavior, suggesting that factors such as mixing regime and residence time maintain steadier oxygen transfer rates.

Extra coarse diffusers, though less efficient than fine bubble diffusers, slightly outperformed coarse bubble diffusers, suggesting that variables such as bubble dispersion patterns, diffuser geometry, or liquid contact time significantly influence oxygen transfer efficiency. This highlights the importance of viable technological alternatives given operational or economic constraints.

CONCLUSIONS

Mathematical modeling of oxygenation capacity in wastewater, accounting for air diffuser type, enabled an accurate representation of the temporal evolution of dissolved oxygen through polynomial models fitted to experimental data. These models highlighted key influences on the oxygenation process. Fine-bubble diffusers demonstrated significantly higher oxygen transfer efficiency due to the greater gas-liquid contact area they produce, making them particularly suitable for aqueous environments. However, coarse and extra-coarse bubble diffusers, while slower, provided more stable and predictable results, which can be advantageous in systems where operational stability is a priority. Statistical analysis of diffuser-type-by-time interactions revealed that diffuser type plays a particularly important role during the initial stages of the oxygenation process. This underscores the need to consider both diffuser type and process duration when designing efficient oxygenation systems, as both factors interact significantly to influence overall treatment performance. This study acknowledges limitations that open avenues for future research. The experiments were conducted using synthetic domestic wastewater to ensure controlled and reproducible conditions. However, performance in real wastewater may differ due to contaminants such as surfactants and suspended solids, which can alter bubble coalescence and surface tension, thereby affecting the mass transfer coefficient. Furthermore, the long-term potential for biofilm formation on diffuser surfaces in a real-world setting could impact performance over time. Future work should aim to validate these models using real wastewater and investigate the long-term operational stability of each diffuser type. This approach lays a foundation for future research exploring additional factors affecting oxygen transfer, such as environmental conditions or the physicochemical properties of water.

Author Contributions: A.L.: Conceptualization, Methodology, Formal analysis, Investigation, writing original draft, writing review & editing, O. S.: Validation, Data curation, Writing review & editing, Visualization, Methodology, Software, Validation, Formal analysis, J.C.: Investigation, Resources, Supervision, Project

administration, E.C.: Funding acquisition, Supervision, Software, Data curation, Visualization.

REFERENCES

Arora-Jonsson, S., 2023. The sustainable development goals: A universalist promise for the future. *Futures*, 146, p.103087. [DOI]

Asselin, C., Comeau, Y. and Ton-That, Q.A., 1998. Alpha correction factors for static aerators and fine bubble diffusers used in municipal facultative aerated lagoons. *Water Science and Technology*, 38(3), pp.79–85. [DOI]

Behnisch, J., Schwarz, M., Trippel, J., Engelhart, M. and Wagner, M., 2022. Oxygen transfer of fine-bubble aeration in activated sludge treating saline industrial wastewater. *Water*, 14(12), p.1964. [DOI]

Cao, Y., Zhang, C., Rong, H., Zheng, G. and Zhao, L., 2017. The effect of dissolved oxygen concentration on oxygen diffusion and bacterial community structure in moving bed sequencing batch reactor. *Water Research*, 108, pp.86–94. [DOI]

Cheng, X., Xie, Y., Zheng, H., Yang, Q., Zhu, D. and Xie, J., 2016. Effect of different shapes of air diffuser on oxygen mass transfer coefficients in microporous aeration systems. *Procedia Engineering*, 154, pp.1079–1086. [DOI]

Dey, S., Bhunia, P. and Surampalli, R.Y., 2022. Sustainability assessment of vermifiltration technology for treating domestic sewage: A review. *Journal of Water Process Engineering*, 50, p.103266. [DOI]

Dyagelev, M.Y., Pavlov, I.I., Nepogodin, A.M., Grakhova, E.V. and Lapina, A.A., 2021. The review of aeration systems for biological wastewater treatment. *IOP Conference Series: Earth and Environmental Science*, 839(4), p.042035. [DOI]

Farazaki, M. and Gikas, P., 2019. Nitrification-denitrification of municipal wastewater without recirculation using encapsulated microorganisms. *Journal of Environmental Management*, 242, pp.258–265. [DOI]

Ghodke, P.K. and Reddy, P.V., 2023. Investigation of mass transfer coefficient for absorption column in carbon sequestration studies. *Materials Today: Proceedings*, 76, pp.14–17. [DOI]

Gillot, S., Capela-Marsal, S., Roustan, M. and Héduit, A., 2005. Predicting oxygen transfer of fine bubble diffused aeration systems: Model issued from dimensional analysis. *Water Research*, 39(7), pp.1379–1387. [DOI]

Herrmann-Heber, R., Reinecke, S.F. and Hampel, U., 2020. Dynamic aeration for improved oxygen mass transfer in the wastewater treatment process. *Chemical Engineering Journal*, 386, p.122068. [DOI]

Herrmann-Heber, R., Ristau, F., Mohseni, E., Reinecke, S.F. and Hampel, U., 2021. Experimental oxygen mass transfer study of micro-perforated diffusers. *Energies*, 14(21), p.7268. [DOI]

Hocaoglu, S.M., Insel, G., Cokgor, E.U. and Orhon, D., 2011. Effect of low dissolved oxygen on simultaneous nitrification and denitrification in a membrane bioreactor treating black water. *Bioresource Technology*, 102(6), pp.4333–4340. [DOI]

Khalil, A.S. and Sharshir, S., 2022. Improving the performance of biological tanks in wastewater treatment plants by modifying the conventional ceramic aerator. *Journal of Physics: Conference Series*, 2305(1), p.012026. [DOI]

Lebrun, G., Benaissa, S., Le Men, C., Pimienta, V., Hébrard, G. and Dietrich, N., 2022. Effect of surfactant lengths on gas-liquid oxygen mass transfer from a single rising bubble. *Chemical Engineering Science*, 247, p.117102. [DOI]

Levitsky, I., Tavor, D. and Gitis, V., 2022. Microbubbles, oscillating flow, and mass transfer coefficients in air-water bubble columns. *Social Science Research Network Working Paper Series*, 15(2), pp.45–62. [DOI]

Lu, J., Li, R., Wan, H., Ma, Q., Li, K., Zhu, D.Z., Feng, J., Yan, Z., Sun, G., Yu, J., Tang, X., Xu, H., Xue, J. and Li, P., 2021. Dissolved oxygen transfer along falling water jets with developing surface disturbance. *Journal of Hydro-environment Research*, 38, pp.129–136. [DOI]

Ma, W., Han, Y., Han, H., Zhu, H., Xu, C., Li, K. and Wang, D., 2017. Enhanced nitrogen removal from coal gasification wastewater by simultaneous nitrification and denitrification in oxygen-limited biofilm reactor. *Bioresource Technology*, 244(1), pp.84–91. [DOI]

Newbry, B.W., 1998. Oxygen-transfer efficiency of fine-pore diffused aeration systems: Energy intensity as a unifying evaluation parameter. *Water Environment Research*, 70(3), pp.323–333. [DOI]

Pang, J., Pan, J., Tong, D., Fu, X., Sun, B., Yang, M. and Li, H., 2020. Effects of hydraulic load and intermittent aeration on pollutant removal and greenhouse gas emission in ecological infiltration systems. *Ecological Engineering*, 146, p.105747. [DOI]

Reshma, M.T., Kumar, M.S.M. and Rao, L., 2021. Numerical modelling of oxygen mass transfer in diffused aeration systems using CFD-PBM approach. *Journal of Water Process Engineering*, 40, p.101920. [DOI]

Rosso, D. and Stenstrom, M.K., 2006. Economic implications of fine-pore diffuser aging. *Water Environment Research*, 78(8), pp.810–815.

Skouteris, G., Rodriguez-Garcia, G., Reinecke, S.F. and Hampel, U., 2020. The use of pure oxygen for aeration in aerobic wastewater treatment: A review of potential and limitations. *Bioresource Technology*, 312, p.123595. [DOI]

Xu, J. and Xu, Z., 2022. China sewage treatment engineering issues assessment. *Journal of Cleaner Production*, 377, p.134391. [DOI]